ANALYTICAL DESIGN AND DEVELOPMENT OF A POTATO SLICING MACHINE

Faysal Ahamed[1*], MD Faysal Refat[2], MD Badrul Islam Palash[3], Iftekhar Ahamed Rafee[4]

[1]Department of Mechanical Engineering, Jiangsu University of Science and Technology, Jiangsu, China
Email: faysalahammed.just@gmail.com
[2]Department of Electrical and Electronics Engineering, Leading University, Sylhet, Bangladesh
Email: mdfaysalrefat4@gmail.com
[3]Department of Computer Science and Technology, Jiangsu university of science and technology, Jiangsu, China
Email: badrulislampalash1@gmail.com
[4]Department of Mechanical Engineering, Beibu Gulf University, China
Email: ahmedrafeeiftekhar@gmail.com

Abstract

This study presents the design and development of a portable potato slicer that addresses key limitations in traditional slicing methods, such as low efficiency, high labor intensity, and safety risks. The slicer features an innovative modular design incorporating a Dongles geared motor and a chain-driven slicing mechanism, capable of processing up to 1.5 tons of potatoes per hour. The adjustable blade holder allows for precise control of slice thickness, ranging from 0.5 to 0.7 mm, catering to various industrial and commercial requirements.

Finite element analysis conducted in SolidWorks confirmed the structural integrity and operational reliability of essential components, including shafts and bearings. The use of food-grade stainless steel and SKD11 for all food-contact parts ensures compliance with hygiene standards while reducing contamination risks and accidental injuries. The compact design not only simplifies maintenance and transportation but also minimizes operational costs.

The slicer significantly reduces processing time and manual labor compared to conventional methods, offering enhanced productivity, flexibility, and safety. Key contributions of this work include the introduction of a scalable slicing solution with customizable thickness settings and a robust transmission system that simulates manual slicing with improved consistency. Future advancements could explore automation enhancements, energy-efficient designs, and broader integration with food processing systems, paving the way for more efficient and sustainable food processing technologies

Keywords

Slicer, Potato, Geared motor, Solidwork, AutoCAD, Analysis.

1. Introduction

Potatoes, being the fourth largest food crop globally [1], are cultivated across extensive land regions and exhibit substantial productivity. In recent years, there has been a notable increase in the demand for potatoes due to the expansion of crop planting areas in various countries worldwide. China, being a prominent agricultural nation [2], holds the top position globally in terms of both potato planting area and output. Consequently, potatoes have become a significant constituent of China's dietary composition [3]. Potatoes are commonly utilized in various aspects of daily life, such as food preparation and snacking. They are readily available in supermarkets and vegetable fields. In the field of medicine, potatoes serve as a versatile vegetable, functioning as both a grain and a vegetable [4]. They possess a high content of carbohydrates, vegetable protein, vitamin C, and other essential elements. These constituents are readily absorbed by the human body, resulting in beneficial effects such as nutritional supplementation, spleen and dampness strengthening, as well as blood vessel protection. The efficiency of potato processing is contingent upon the chosen processing method, and the current research will primarily concentrate on enhancing the secondary processing efficiency of potatoes. Potatoes undergo many stages of processing prior to utilization, including washing, peeling, slicing/dicking, and other essential procedures. The conventional potato processing technique is performed manually, resulting in a lengthy duration and limited efficiency. Additionally, prolonged physical labor poses a risk of hand injuries and additional hazards. The quality of slicing plays a crucial role in the processing process, as it directly impacts the taste of the final product. Therefore, it is imperative to conduct research on the structural design of potato slicer in order to address the issue of low efficiency in potato processing.

The present study focuses on the design of a portable potato slicer. After conducting an extensive review of literature and analyzing the structural models of different slicer types, it was ultimately determined that the equipment should be categorized into three distinct components: the feeding mechanism, the slicing mechanism, and the unloading mechanism. The potato undergoes transportation to the slicing actuator via a conveyor belt in the feeding mechanism. Subsequently, the potato is introduced into the drum grid of the actuator in a sequential manner. The drum rotates and exerts force on the potato, propelling it through the stationary knife holder. The potato slice is then output from the unloading device positioned beneath the knife holder. Computer-aided design software is extensively utilized in the design calculation and modeling simulation process, significantly enhancing design efficiency. To guarantee the safety of food processing, the equipment's elements and components that will directly interact with potatoes are specifically built to be processed using materials that adhere to the requirements for safe food processing.

2. Materials & Methods

2.1. Design Ideas

The necessary information of the potato slicer was consulted in accordance with the structural design requirements. It was found that the majority of existing potato slicers are integrated, resulting in low processing efficiency and inadequate equipment safety. The primary objective of the structural design of the portable potato slicer is to develop a compact and framework that is user-friendly, easily maintainable, exhibits high operational efficiency, maintains high processing quality, and enables the pre-processing of potato chips with varying thicknesses through blade replacement or adjustment. It significantly decreases the amount of work required by kitchen staff and effectively prevents the unintended harm caused by using conventional knives for food preparation. The first configuration involves choosing a motor with a power output of around 1200W 48V DC Servo Motor, 4.5 Nm, 2500 rpm. The slice specification is set to range from 5 to 7 millimeters. Following extensive comparisons and meticulous investigation, a decision was made to partition the potato slicer's structure into three distinct components: the feeding mechanism, the slicing mechanism, and the unloading mechanism [5]. Additionally, a conveyor belt was employed at the center to facilitate the transfer of potatoes at different time intervals. The adoption of the modular combination design approach aims to enhance the compactness and lightweight nature of each component. Additionally, each module is fitted with locking universal wheels to promote convenient daily mobility. To minimize the overall weight of the machine, it is advisable to incorporate square pipes, castings, or counterweights in specific locations to facilitate connection and fixation. This will enhance the structural integrity and stability of the equipment during operation. The remaining locations that will come into direct or indirect contact with the processed potatoes will be equipped with sheet metal parts made of 304 stainless steel, while the conveyor belt will be constructed using food-grade PVC. By implementing this approach, the safety of food processing may be significantly ensured. Additionally, a clear cover can be affixed to the processing equipment during subsequent stages to prevent any foreign objects from falling. Additionally, this feature serves to prevent the operator's fingers or hair from inadvertently interfering with the transmission of the device. The potato slicer's structure is relatively uncomplicated, with significance placed on the design of the slicing scheme and the selection of the transmission scheme for the slicing part. Consequently, two schemes are suggested.

2.2. Motor Selection Scheme

To choose a suited motor for an application, there are several important factors which should be considered. This paper explains how an ideal motor is selected, and it is based on the information from the following sources. Torque and load requirements: knowing the torque requirement, that is starting,

running and stall torque, this can ensure that the chosen motor can perform the task. This information would not only help select the torque for the application but also can tell what load the motor should be able to accelerate if he knows what torque the motor provides [6].

1. Speed requirements: this would specify the speed range of the application and it can be also used to decide the motor speed if there is some gearing or pulley system to make the motor's speed down
2. Select of the motor itself: AC or DC motor: this can be selected depending on power available at the place of use and the requirement of its control
3. Stepper, Servo, other specialized motors: these types are used to motors which would be desired to control the position and the speed exactly so, using these types depending on the conditions
4. Power and efficiency: check the power rating to see if the motor can work the requirement power and evaluate the energy cost of the motor
5. The size and mounting: check the size and the weight of motor to see if it suitable for certain application and if the sufficient mounting option is available
6. The environment: check to see if the motor can live an in a given environment. For example, the motor must be required to have special enclosure if it will be used in hot or cold weather or outside where should be presenting dust, water or corrosive chemicals
7. Motor drive and control system: this would specify what kind of control system should work with the motor, such as VFD for AC motor and controller for the others. And it can save some costs if the motor system would also drive some feedback system, such as using the motor with the built-in motor hall effect or an encoder
8. Cost effectiveness: while some motor is expensive to buy others consumes more energy.
9. Regulatory and standard: the motor would be chosen always concerning the law steps to promote the motors such as efficiency or the other.

In conclusion, be familiar to these factors and with taking into consideration all the above steps would guarantee to choose a suited motor for certain application.

2.3. SERVO Motor selection

1. Housing: acts as a first defense and protection of the internal components of the motor. It is usually made from aluminum, and the structure allows for easy assembly and disassembly.

2. Stator: the stationary part of the servo motor, which consists of a stack of slotted laminations to be wound by copper wire into a certain pattern. It complements the magnet on the rotor and determines the electrical characteristics of the motor.
3. Rotor: the working part of the servo motor that includes a shaft with a number of magnet segments attached to it or embedded in a stack of laminations attached to the shaft. When the magnetic flux flows between and out of the magnet sections, it interacts with the electromagnetic fields generated by the stator to create rotation.
4. Motor shaft: responsible for transferring the electric energy to the machine moved by the motor. It is traditionally made of cold or hot-rolled steel, and the shaft can be connected to a gearbox and motor combination, a belt and pulley combination, or a direct drive.
5. Bearings: the components are used to allow the rotor to spin relatively smoothly in the stator. They are designed to support the rotor and ensure minimal vibration and maximum precision, effectiveness, and smoothness.
6. Feedback system: the electro-mechanical device that communicates the motor's speed and direction back to the drive to ensure proper positioning and speed control.
7. Cooling system: optional component that helps maintain an optimal temperature level, which is especially important in high-power applications without overheating.
8. Servo controller: an element that ensures that the motor and the digital control element mesh by converting signals appropriately.
9. Power connection: the component is responsible for providing the needed electrical energy for the operation of the motor. The type of power depends on the specific motor model.

3.1. Design and calculation of chain transmission mechanism

3.1.1. Calculation of transmission parameters

Table 3-3 in "Comprehensive Training in Mechanical Design" [7], edited by Wang Mingqiang and Zhu Yongmei, displays the range of values for common mechanical transmission and support efficiencies. The roller chain has a transmission efficiency of 0.96, denoted as η_1. The transmission efficiency of ball bearings used in pairs is denoted by the symbol η_2 and has a value of 0.99. The book "Engineering Mechanics" [8], edited by Gu Chengjun, Jiang Yijun, and Liao Dongbin, provides a formula (6-1) to determine the torque, power, and speed of each axis.

$$T = m = 9550\frac{P}{n} \qquad \text{eq.1}$$

In the formula:

T——Torque, N·m.

n——Rotation speed, r/min.

P——On-axis power, kW.

As per the Eastern calendar, the motor PF18-0200-30S has been chosen in section 3.1 for the selection and calculation of transmission belt reduction motor. The motor specifications are inputted into eq.1 to compute the torque T_0 of the motor shaft.

$$T_0 = 9550\frac{P_0}{n} = \frac{9550\times0.2}{46} = 41.50N\cdot m \qquad \text{eq.2}$$

Because the transmission ratio i=1, n_1=46r/min, η_1=0.96, the power and torque transmitted on the belt roller shaft are calculated:

$$P_1 = P_0\cdot\eta_1 = 0.2\times0.96 = 0.192kW \qquad \text{eq.3}$$

$$T_1 = 9550\frac{P_1}{n_1} = \frac{9550\times0.192}{46} = 39.86N\cdot m \qquad \text{eq.4}$$

3.1.2. Design and verification of chain drive of transmission mechanism

The basic configuration of the transmission mechanism chain drive sets the number of teeth on both the large and small sprockets to Z_1=Z_2=21. As stated in Table 13-2-6 of the third edition of "Modern Mechanical Design Handbook" edited by Qin Datong and Xie Liyang [9], The book contains the coefficient K_A for assessing working conditions. The value of K_A is determined to be 1. Next, compute the design power P_d using the given formula:

$$P_d = K_A\cdot P = 1\times0.2 = 0.2kW \qquad \text{eq.5}$$

In the formula:

K_A——working condition coefficient.

P——power, kW.

Calculate the power P_0 transmitted by a single row of chains under specific conditions:

$$P_0 = \frac{P_d}{K_Z K_P K_L} \qquad \text{eq.6}$$

In the above formula, K_Z represents the coefficient for the number of teeth on the tiny sprocket.

K_p is a ranking coefficient. The K_L coefficient represents the length of the chain.

The book "Modern Mechanical Design Handbook" edited by Qin Datong and Xie Liyang provides

information on the tiny sprocket tooth number coefficient K_Z and chain length coefficient K_L in Table 13-2-7 of its third volume.

$$K_Z = \left(\frac{Z_1}{19}\right)^{1.5} = \left(\frac{21}{19}\right)^{1.5} = 1.16 \qquad \text{eq.7}$$

$$K_L = \left(\frac{L_P}{100}\right)^{0.5} = \left(\frac{42}{100}\right)^{0.5} = 0.65 \qquad \text{eq.8}$$

The coefficient K_p is ranked in Table 13-2-8 of the third volume of "Modern Mechanical Design Handbook" edited by Qin Datong and Xie Liyang. The table indicates that K_p has a value of 1. Apply the given data as input to eq.6 in order to calculate:

$$P_0 = \frac{P_d}{K_Z K_P K_L} = \frac{0.2}{1.16 \times 1 \times 0.65} = 0.27kW \quad \text{eq.9}$$

Calculate the power P_0=0.27kW and rotational speed n_1=46r/min conveyed by the single-row chain. Subsequently, identify the appropriate chain based on the third volume of "Modern Mechanical Design Handbook" edited by Qin Datong and Xie Liyang, and figure 13-2-8 in the book. The number is 08A. Refer to table 13-2-2 in order to choose the chain pitch with a value of P=12.7mm.

Verify the diameter d_k of the shaft hole of the tiny sprocket.

$$d_k \leq d_{kmax} \qquad \text{eq.10}$$

The maximum permissible diameter of the shaft hole, denoted as d_{kmax}=47mm, can be obtained by referring to Table 13-2-9 in Volume 3 of the "Modern Machinery Design Manual".

$$d_k \leq 47\text{mm} \qquad \text{eq.11}$$

Calculate the initial center distance a_0:

$$a_0 \geq 0.2Z_1(i+1)P \qquad \text{eq.12}$$

$$\geq 0.2 \times 21 \times 2 \times 12.7$$

$$\geq 106.68mm$$

Initial center distance a_{0P} calculated in terms of pitch:

$$a_{0P} \geq \frac{a_0}{P} \qquad \text{eq.13}$$

$$\geq \frac{106.68}{12.7}$$

$$\geq 8.4$$

Typically, the value of a_{0P} ranges from 30P to 50P. It is now determined that the minimum distance between centres must exceed 8.4P. Based on the current structural dimensions of 8.4P, it does not satisfy the design specifications and should be increased accordingly. Ultimately, the initial distance between the centres is determined. The distance between point A and point P is equal to 15 times the value of P.

Determine the quantity of chain links, denoted as L_P:

$$L_P = \frac{Z_1+Z_2}{2} + 2a_{0P} + \frac{k}{a_{0P}} \qquad \text{eq.13}$$

$$= \frac{21+21}{2} + 2 \times 15 = 51$$

Determine the value of the variable L_P, which represents the number of chain links, as 51. To ensure an even number of links, we will round the number of links to the next even number. In this case, we have L_P=52. Let's calculate the chain length, L:

$$L = \frac{L_P \cdot P}{1000} = \frac{52 \times 12.7}{1000} = 0.66m \qquad \text{eq.14}$$

Calculate the center distance a_c:

$$a_c = \frac{P}{2}(L_P - Z) = \frac{12.7}{2} \times (52 - 21) = 196.85mm \qquad \text{eq.15}$$

Calculate the actual center distance a:

$$a = a_c - \Delta a = 196.85 - 0.004 \times 196.85 = 196.1mm \qquad \text{eq.16}$$

Calculate the chain speed v:

$$v = \frac{Z_1 n_1 P}{60 \times 1000} = \frac{21 \times 46 \times 12.7}{60 \times 1000} = 0.2m/s \qquad \text{eq.17}$$

Calculate the effective circular force F_t:

$$F_t = \frac{1000P}{v} = \frac{1000 \times 0.2kW}{0.2} = 1000N \qquad \text{eq.18}$$

Calculate the force F acting on the axis:

$$F = 1.15K_A \cdot F_t = 1150N \qquad \text{eq.19}$$

The third edition of the "Modern Machinery Design Manual" cites Figure 13-2-5, Table 13-2-47, and Table 13-2-48 as references for the appropriate selection of the lubrication method. Regularly employ a brush or oil bottle to manually eliminate loose chains. Apply oil to the space between the inner and

outer chain plates.

Determine the static strength of the roller chain using the formula (13-2-1) provided in the book.

$$n = \frac{F_u}{K_A F_t + F_c + F_f} \quad \text{eq.20}$$

In the formula:

n——Static strength safety factor.

F_u——chain ultimate tensile load, kN.

F_t——effective circular force, kN.

F_c——The force caused by centrifugal force, kN.

q——chain quality, kG.

v——Chain speed, m/s.

F_f hanging force, whichever is greater between F_f' and F_f''.

$$F_f' = \frac{K_f q a}{100} = \frac{2.7 \times 0.6 \times 196.1}{100} = 3.18N \quad \text{eq.21}$$

$$F_f'' = \frac{(K_f + \sin\theta) q a}{100} = \frac{(2.7 + \sin 60°) \times 0.6 \times 196.1}{100} = 4.2N \quad \text{eq.22}$$

K_f——coefficient.

a——Chain drive center distance, mm.

θ——The inclination angle between the center line of the two wheels and the horizontal plane.

n_p——allowable safety factor, n_p=4~8.

The third volume of "Modern Mechanical Design Handbook" states that Table 13-2-2 displays the value of F_u as 13.9kN. The parameters derived earlier are utilised in formula (3.28) to compute:

$$n = \frac{F_u}{K_A F_t + F_c + F_f} = 13.8 > n_p \quad \text{eq.23}$$

Calculate the static strength of the roller chain according to the formula (13-2-3) in the book:

$$T = \left(\frac{K_P P_o'}{K_A P}\right) \cdot \frac{L_P}{100} \quad \text{eq.24}$$

In the formula:

T——service life, h.

Z_1——The number of small sprocket teeth.

n_1——small sprocket speed, r/min.

K_P——Multi-row chain number coefficient.

K_A——working condition coefficient.

L_P——Chain length, mm.

K_P is determined as 1 by referring to the row coefficient table in Table 13-2-8 in the book. Similarly, K_A is determined as 1 by referring to the working condition coefficient table in Table 13-2-6 in the book. These acquired parameters are then plugged into eq.24 for calculation.

$$T = \left(\frac{K_P P_o'}{K_A P}\right) \cdot \frac{L_P}{100} = 15000 \times \frac{1\times0.32}{1\times0.2} \times \frac{52}{100} = 12480h \quad \text{eq.25}$$

Determine the level of resistance to wear exhibited by a roller chain:

$$T = 91500\left(\frac{C_1C_2C_3}{P}\right) \cdot \frac{L_P}{v} \cdot \frac{Z_1 i}{i+1}\left(\frac{\Delta p}{P}\right)\frac{P}{3.2d_2} \quad \text{eq.26}$$

In the formula:

C_1——wear coefficient, check Figure 13-2-8 to get C_1=5;

C_2——pitch coefficient, look up table 13-2-13 and get C_2=1.44;

C_3——number of teeth-speed coefficient, check Figure 13-2-9 and get C_3=1;

Put the parameters and related calculation parameters obtained from the table lookup into formula (3.34) to calculate:

$$T = 91500\left(\frac{5\times1.44\times1}{32}\right) \cdot \frac{52}{0.2} \cdot \frac{21}{1+1} \times 0.03 \times \frac{12.7}{3.2\times3.98} = 85118h \quad \text{eq.27}$$

3.1.3. Computation of fundamental characteristics of a sprocket

Based on the previously determined sprocket characteristics and table lookup, the number of teeth on the sprocket is $\boldsymbol{Z_1}$=21, the chain pitch is P=12.7mm, and the maximum diameter of the chain's roller is $\boldsymbol{d_1}$=7.92mm.

Determine the indexing circle diameter (d), tooth tip circle diameter ($\boldsymbol{d_a}$), and tooth root circle diameter ($\boldsymbol{d_f}$) based on the fundamental characteristics and primary dimensions provided in Table 13-2-14 for the sprocket.

$$d = \frac{P}{\sin\frac{180^\circ}{Z}} = \frac{12.7}{\sin\frac{180^\circ}{21}} = 85.21mm \quad \text{eq.28}$$

$$d_a = P\left(0.54 + \cot\frac{180^\circ}{Z}\right) = 12.7 \times \left(0.54 + \cot\frac{180^\circ}{21}\right) = 91.12mm \quad \text{eq.29}$$

$$d_f = d - d_1 = 85.21 - 7.92 = 77.29mm \quad \text{eq.30}$$

Calculate the chain length L:

$$L = \frac{L_P \cdot P}{1000} = \frac{60\times25.4}{1000} = 1.52m \quad \text{eq.31}$$

Add the following to the centre distance a_c calculation:

$$a_c = P(2L_P - Z_1 - Z_2)K_a = 520.45mm \quad \text{eq.32}$$

Calculate the actual center distance a:

$$a = a_c - \Delta a = 520.45 - 0.004 \times 520.45 = 518.37mm \quad \text{eq.33}$$

Calculate the chain speed v:

$$v = \frac{Z_1 n_1 P}{60 \times 1000} = \frac{17 \times 56.8 \times 25.4}{60 \times 1000} = 0.41m/s \quad \text{eq.34}$$

Calculate the effective circular force F_t:

$$F_t = \frac{1000P}{v} = \frac{1000 \times 2.2kW}{0.41} = 5365.85N \quad \text{eq.35}$$

Calculate the force F acting on the axis:

$$F = 1.15K_A \cdot F_t = 6170.73N \quad \text{eq.36}$$

The third edition of the "Modern Machinery Design Manual" cites Figure 13-2-5, Table 13-2-47, and Table 13-2-48 as references for the appropriate selection of the lubrication method. Regularly employ a brush or oil bottle to manually eliminate any loose chains. Apply oil to the space between the inner and outer chain plates.

3.1.4. Shaft design and verification

There are three primary techniques for determining the strength of a shaft: evaluation of permissible shear stress, evaluation of permissible bending stress, and assessment of safety factor. These three strategies can be employed either separately or consecutively. In general, the calculation of the spinning shaft based on the permissible bending stress is sufficiently reliable and does not necessarily require verification using the safety factor approach. When the strength calculation fails to fulfil the specified requirements, it is necessary to modify the structural design. These two aspects often work together and intersect with each other [10]. The belt roller shaft of the gearbox mechanism is constructed from 45 steel, while the actuator utilises 40Cr as the material for preliminary design verification. When a keyway is present on the shaft, the diameter of the shaft should be expanded accordingly: by 3% for single keys and by 7% for double keys.

- Transmission mechanism transmission belt shaft

The solid shaft shear stress can be calculated using formula (16.1) from the fourth edition of "Mechanical Design" edited by Qiu Xuanhuai.

$$\tau_T = \frac{T}{W_T} = \frac{9.55\times10^6 P/n}{0.2d^3} \leq [\tau_T] \text{ MPa} \qquad \text{eq.37}$$

Once the formula is distorted, the design formula can be derived, allowing for the calculation of the minimal shaft diameter that satisfies the requirements of strength design.

$$d \geq \sqrt[3]{\frac{9.55\times10^6 P}{0.2[\tau_T]n}} = C\sqrt[3]{\frac{P}{n}} \text{ mm} \qquad \text{eq.38}$$

In the formula:

W_T——The torsional section coefficient of the shaft, mm^3.

τ_T - torsional shear stress, MPa.

$[\tau_T]$ ——Allowable torsional shear stress, MPa.

P——The power transmitted by the shaft, kW.

n——The rotation speed of the shaft, r/min.

d——The diameter of the shaft, mm.

T——The torque of the shaft, N·mm.

C——Coefficient related to shaft material.

Based on the coefficient C provided in Table 16.2 of the fourth edition of 'Mechanical Design' edited by Qiu Xuanhuai, the calculation involves using the value of C=106 for 45 steel, the shaft speed n=46r/min for the gearbox belt, and the power P=0.192kW transmitted on the shaft. These values are plugged into formula (3.61) for calculation.

$$d \geq C\sqrt[3]{\frac{P}{n}} = 106 \times \sqrt[3]{\frac{0.192}{46}} = 17.07\text{mm} \qquad \text{eq.39}$$

The shaft will experience deformation when subjected to a load. Shaft deformation can be categorised into three types: deflection, rotation angle, and torsion angle. The acceptable torsion angle for precision machinery shafts is between 0.15°/m and 0.3°/m. For common gearbox shafts, the acceptable torsion angle is from 0.5°/m to 1°/m. Accuracy The permissible torsion angle for the lower shaft is between 1°/m and 2°/m. The torsion angle calculation formula per unit shaft length, as stated in the fourth edition of "Mechanical Design" edited by Qiu Xuanhuai, is given by the equation 16.8.

$$\frac{\varphi}{l} = \frac{T}{GI_P} \leq [\varphi] \quad \text{eq.40}$$

Once the formula is altered, the design formula may be derived, allowing for the calculation of the minimal shaft diameter that satisfies the stiffness design criteria.

$$d \geq \sqrt[4]{\frac{32\times|T|_{max}\times180}{G\times\pi^2\times[\varphi']}} \qquad \text{eq.41}$$

In the formula:

d——The diameter of the shaft, mm.

$[\varphi']$—Allowable torsion angle per unit length, °/m.

$|T|_{max}$——maximum torque, N·m.

G——Shear elastic modulus of shaft material, GPa.

I_P——polar moment of inertia of shaft section, m4.

The mechanical design handbook states that the shear elastic modulus of 45 steel is G=80GPa, the permitted shear stress is [τ]=40GPa, and the proposed allowable torsion angle per unit length is [φ^']=2°/m. Input the eq.41 for calculation:

$$d \geq \sqrt[4]{\frac{32\times39.86\times180}{80\times10^9\times\pi^2\times2}} = 19.53\text{mm} \qquad \text{eq.42}$$

The shaft end diameter of the belt roller shaft is rounded to 20mm based on the design calculations of strength and stiffness, as well as the selection of supporting bearings and specifications for the shaft diameter.

Check the strength of the shaft:

$$W_P = \frac{\pi d^3}{16} = \frac{\pi\times20^3\times10^{-9}}{16} = 1.57\times10^{-6}\text{m}^3 \qquad \text{eq.43}$$

$$\tau_{max} = \frac{T}{W_P} = \frac{39.86}{1.57\times10^{-6}} = 25.39\text{MPa} < [\tau] = 40\text{MPa} \qquad \text{eq.44}$$

Check the stiffness of the shaft:

$$I_P = \frac{\pi d^4}{32} = \frac{\pi\times20^4\times10^{-12}}{32} = 1.57\times10^{-8}\text{m}^4 \qquad \text{eq.45}$$

$$\varphi' = \frac{T}{GI_P}\times\frac{180}{\pi} = \frac{39.86}{80\times10^9\times1.57\times10^{-8}}\times\frac{180}{\pi} = 1.82°/\text{m} < [\varphi'] = 2°/\text{m} \qquad \text{eq.46}$$

In summary, the parameter design of the shaft meets the design requirements.

3.2. Key Component of Designing Parts

1. Power Transmission

Shafts transmit mechanical energy from motors to blades. Source 1200W 48V DC Servo Motor, 4.5 Nm, 2500 rpm spins a shaft via chain spoke, efficiently conveying power for slicing. Well-designed shafts ensure smooth, uninterrupted energy transfer for top performance.

2. Maximized Productivity

A shaft's design influences efficiency and capacity. Source 2's machine achieves over 80% efficiency partly from its shaft and transmission system, demonstrating how components contribute significantly to overall function. In closing, shafts play vital mechanical roles in potato slices, from power handling to structural dependability [11]. Their optimization, revealed in documentation, is critical for top output and satisfaction of processing needs.

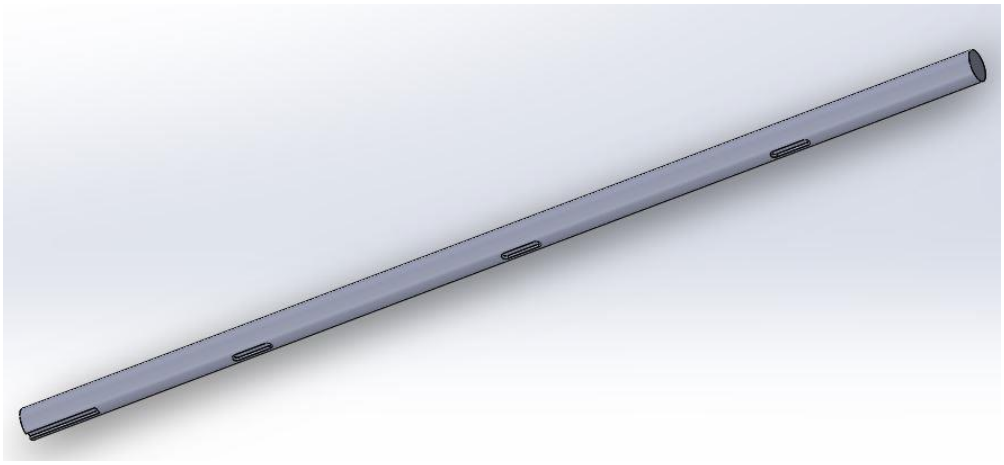

Fig.1. 3D Shaft.

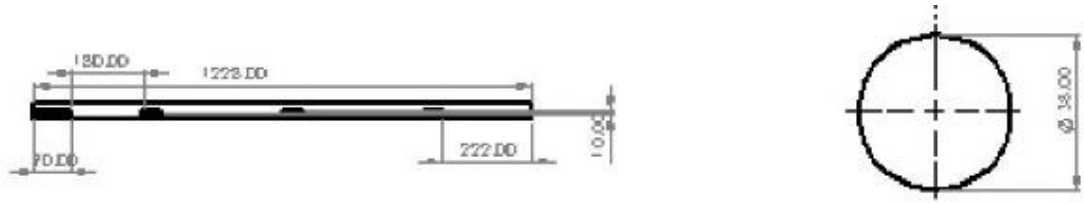

Fig.2. 2D Shaft.

3. Orientation and Movement

A potato slicing machine might have the slice axis horizontal or vertical, designed depending on whether the machine is set vertically or horizontally. This orientation affects the direction by which the potatoes move against a stationary or moving blade or set of blades.

When slicing horizontally, the potatoes might be thrown in across a conveyor belt of moving potatoes across the stationary blades or set of blades that are moving compelled by mechanical cutters.

4. Blade Herding and Blade Interaction

The blades might be fixed into the slice axis slots across the potatoes. Blade sharpness and angle must be precise to acquire a deliciously sharp cut while maintaining vertical alignment for best and consistent starch cut quality [12].

Mechanical forces in variance might be used in propelling the potatoes against the blades.

5. Quality and Control of Slice Thickness

The gap between preset programmed blades must be itself precisely constant. The real blade might be able to move up and down or be easily changed when the edge is getting blunt so that a constant quality of the slice is achieved. Optic sensors accurately ensure that the size of the quantity of slice remains constant and quality. The motor slicer will then be set to cut at a programmed power level. The uniformity of thickness is maintained as slicing is also at a constant power level and the same rigid tools and advantages are used to slice from a higher cut the hard potato or a softer aborigine.

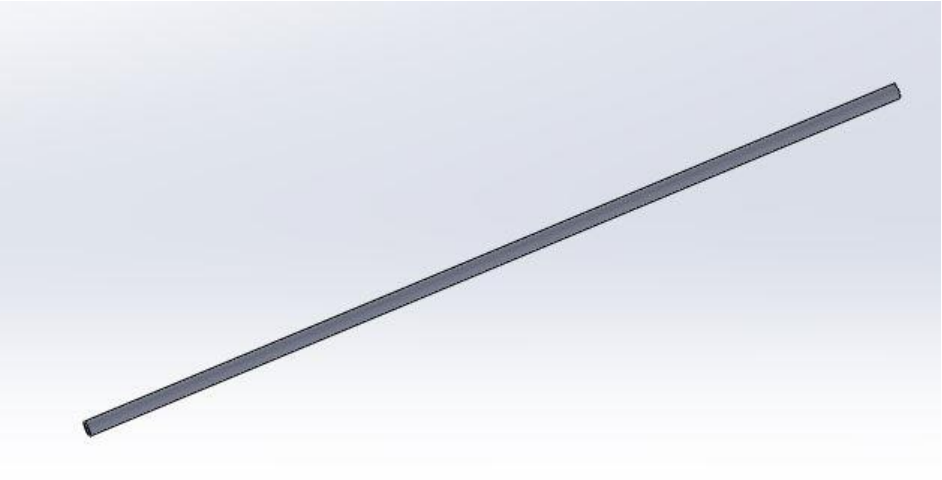

Fig.3. 3D Slicing Axis.

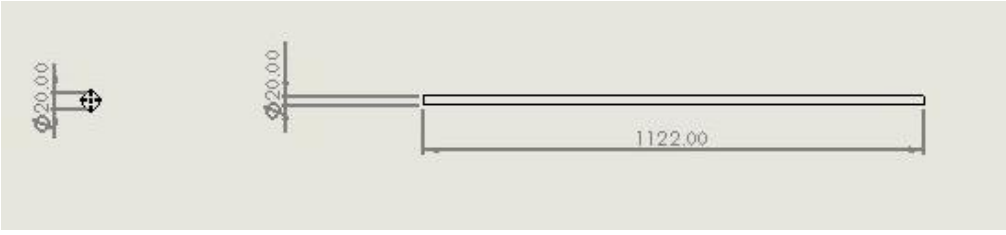

Fig.4. 2D Slicing Axis.

6. Slicing blade

The intricacies of the slicing mechanism at the heart of a potato slicer involve several critical mechanical components arranged to expeditiously partition potatoes into congruent segments. Upon

inspection of the provided sources, here is an elaborated depiction of how the slicing blade performs within a potato slicer

7. Cutting Action

The fundamental cutting action involves a keen edge of the blade making contact with the potato. The exertion either by the potato's movement against the blade or by the blade's movement through the potato causes a clean severance, splitting the potato into slices or other shapes. The thickness of the slices is predetermined by the distance between the blades or the depth of the cut set by the apparatus's settings.

8. Efficiency and Uniformity

The design of the blade and the precision of the apparatus's mechanical systems ensure that each slice is uniform in thickness, which is crucial for the quality of the final product. The competence of the apparatus, as noted in Source is also a critical factor, with machines accomplishing high capacities and maintaining good uniformity in slice thickness.

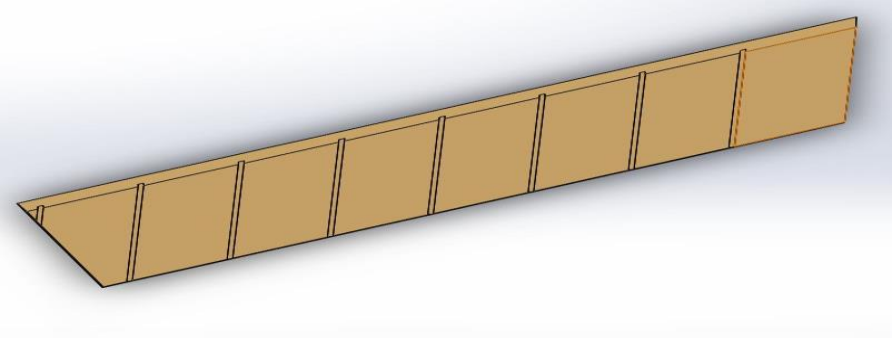

Fig.5. 3D Slicing Blade.

3.3. Assembly Process

Frame Construction: The first step is consolidation of the frame, or mainframe using the materials determined. The frame should provide a secure and sturdy platform onto which other components can be mounted.

Mounting the Motor: Secure the Servo motor the motor base. Ensure that the motor is well aligned with the spoked system for efficient transmission of power.

Installing the Slicing Unit: Secure the slicing shaft and the idler shaft onto the frame. Mount the slicing unit onto the frame and pay special attention to how the blades are set up.

Assembling the Holler: the top of the Holler, install where the potatoes will be deposited. At the bottom, attach the outlet, which will lead the sliced potatoes to the collection point.

Final assembly: Install the spoked and the bearing system such that it is running between the motor Spoked and the slicing unit Gear. Ensure that the Chain spoked system is well connected to ensure efficiency in power transmission. Ensure that all moving parts are sufficiently moves freely.

The assembly design was efficient as every other component is designed by an industrial designer and well connected through screws or welded in place. With a focus on potato, through development of components, which ensure regulated load focalization and slicing efficiency and incorporated onto the frame, formed an efficient slicer suitable for a cottage industry in a food and restaurant as well as for other farms for the processing of the respective energy giving crops.

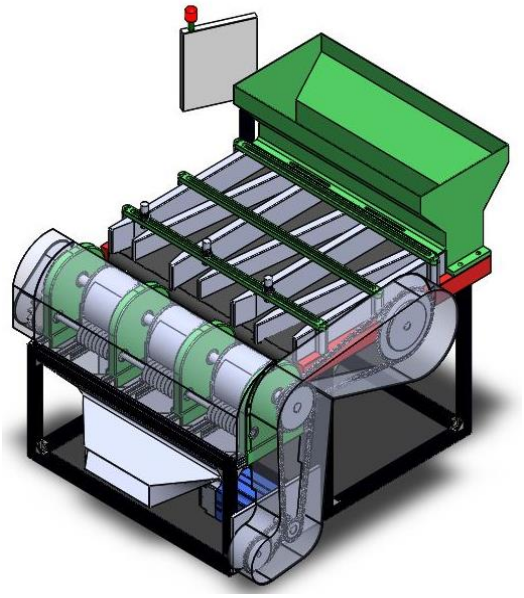

Fig.6. Potato Slicer Assembly Design.

3.4. Finite Element Analysis

3.4.1. Finite element analysis of Pressure Fan

Objective: To analyze the strain Analysis, Displacement Analysis, Safety and Strain Analysis deformation of the Pressure Fan operational loads.

The Pressure Fan are modeled in 3D using CAD software and imported into the Solidwork software. Material properties is SKD11.Boundary conditions and loads are applied to simulate the forces experienced during slicing.

The stress distribution shows high-stress concentrations at the edges and mounting points of the Pressure Fan. the maximum stress on the Pressure Fan is 1.651×10^{8} N/m², which is far less than the maximum yield stress of 2.827×10^{8} N/m², which meets the design requirements

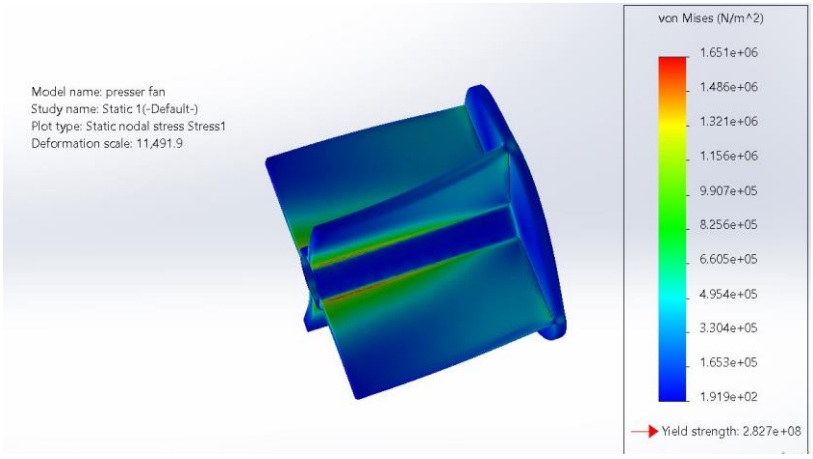

Fig.7. Fan Finite Element Analysis Stress Diagram.

Strain analysis the maximum unit length deformation on the Fan is 6.078, and the strain area and the strain value is too High and almost the design requirements. The results are used to optimize the Fan thickness and material selection to ensure durability.

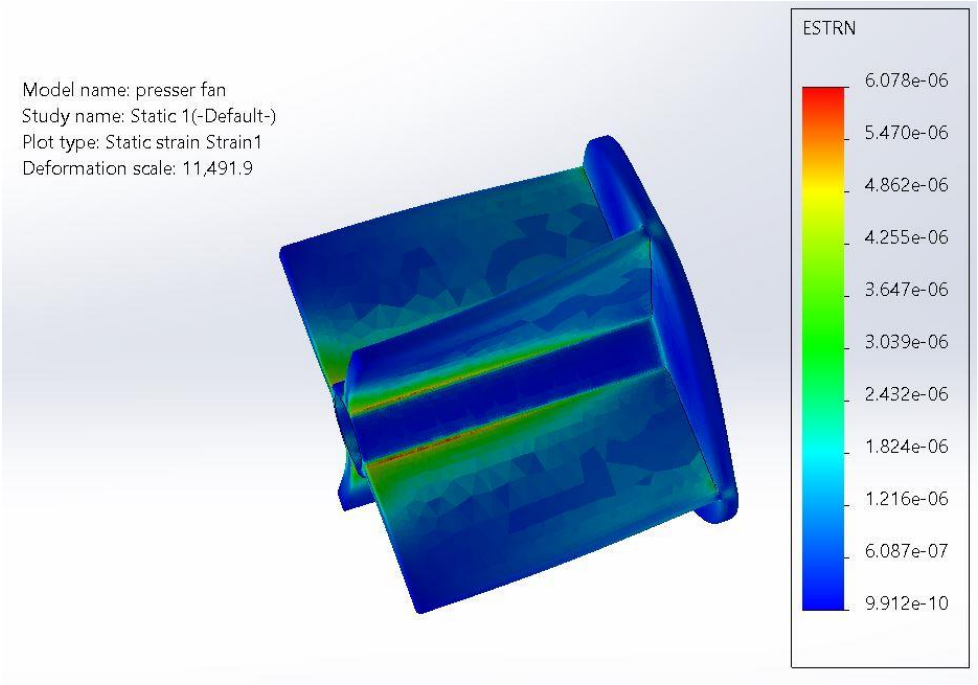

Fig.8. Fan Finite Element Analysis Strain Diagram.

The factor of safety analysis image can be seen that the minimum value of the safety factor on the Fan maximum safety factor reached $S=1.473\times10^5$. Combined with these finite element analysis results, the overall structure of the Fan can meet the safe.

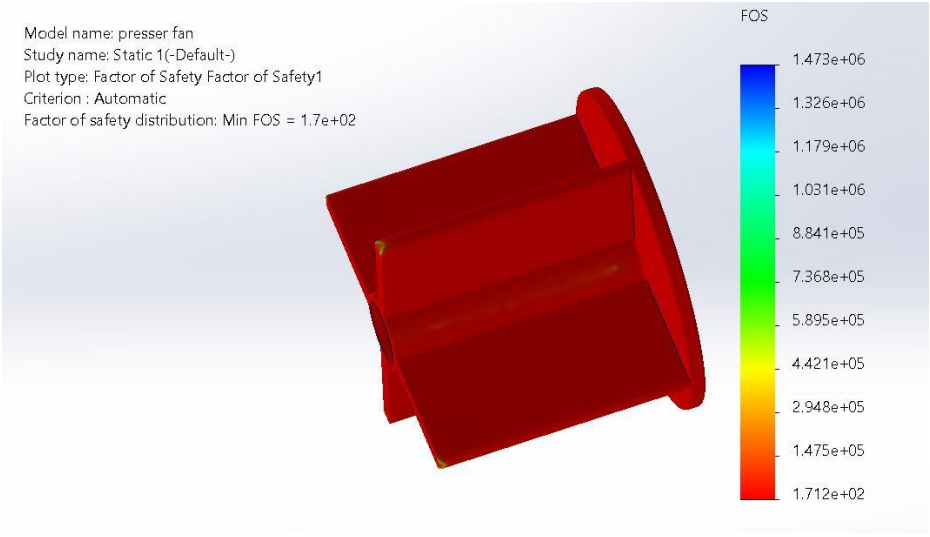

Fig.9. Fan Finite Element Analysis Safety Diagram.

The Displacement Analysis of the Pressure Fan in the displacement analysis diagram shows the deformation of the Fan load. The diagram highlights areas of maximum displacement are 1.473mm the displacement critical for understanding and mechanical behavior of the Fan.

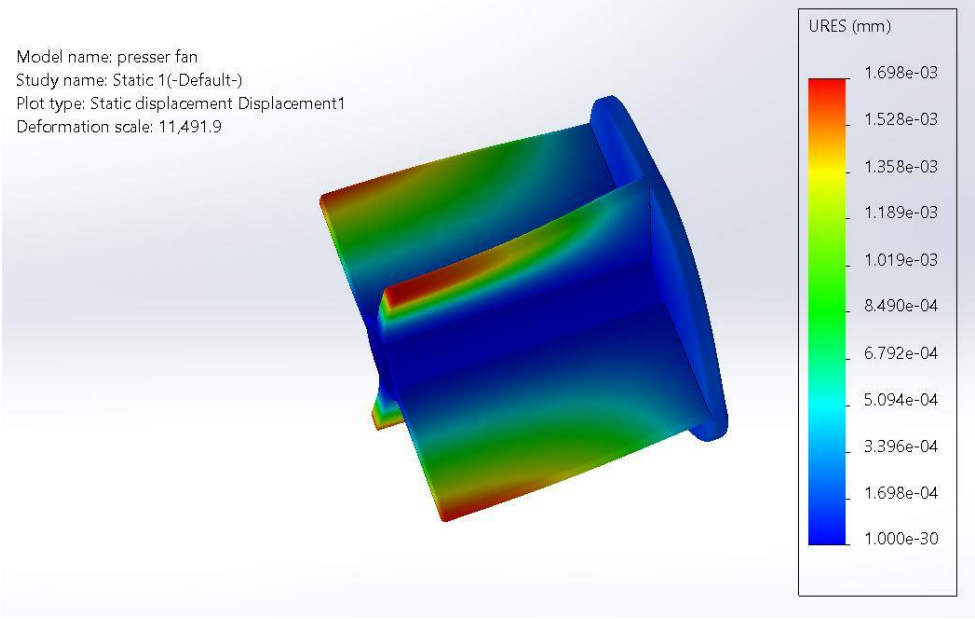

Fig.10. Fan Finite Element Analysis Displacement Diagram.

3.4.2. Finite element analysis of Shaft

- Shaft Analysis: Strain, Stress, Safety, and Displacement

Being one of the main elements in a potato slicing machine, the shaft is responsible for transmitting power from the motor to the cutting blades. As a result, analyzing the shaft in terms of strain, stress,

safety, and displacement is crucial to check its reliability. Below is a more detailed description of the analysis along with minimum and maximum values.

- Strain Analysis

To define the deformation type and the current behavior of the shaft under loads.

Material Properties: introduce the properties of the material MILD steel J:195,000 N/mm^2, Y: 110,000 N/mm^2 G: 80,000 N/mm^2

Boundary Conditions and Loads: try to apply both tensile load. Apply any type of load or sequences of loads that are known o cause strains in shafts.

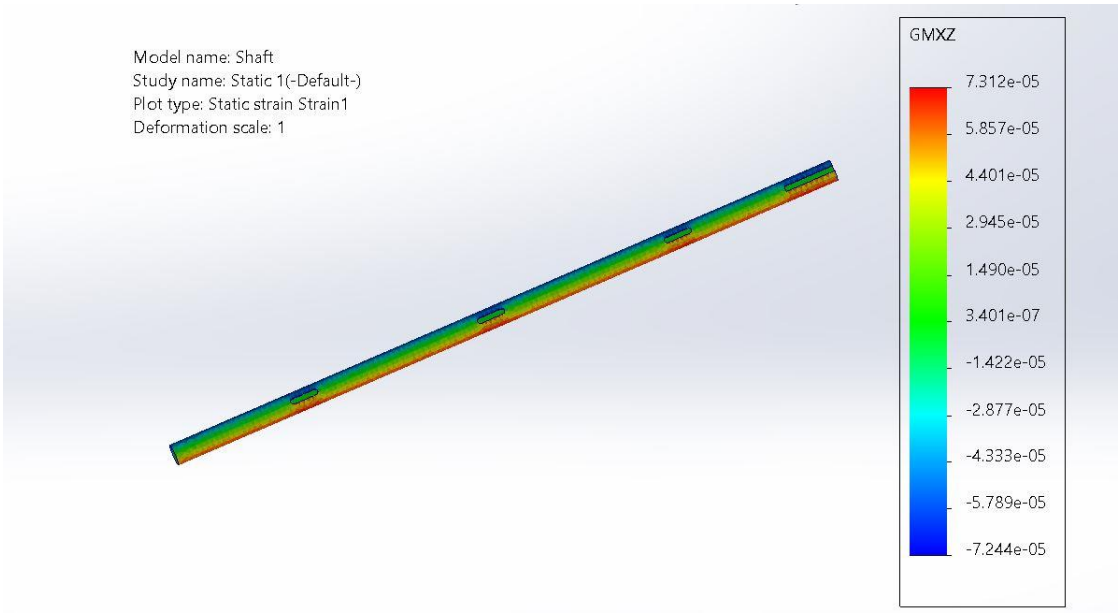

Fig.11. Shaft Finite Element Analysis Stain Diagram.

- Stress Analysis

To define the distribution of the stress in the shaft under specified loads.

Methodology:

Modeling: The shaft is modeled and divided by the mesh.

Material Properties: the quality of the material often has to be determined (mild steel) and its yield strength. The same parts are to be applied and introduced.

Minimum Stress: The minimum stress always occurs at the center of the shaft since the load has to be applied far from these areas.

Strain: The strain is minimum at the supported or the fixed points as these points will have the least stress which would not create any strain. The strain is maximum at the high stress concentration points.

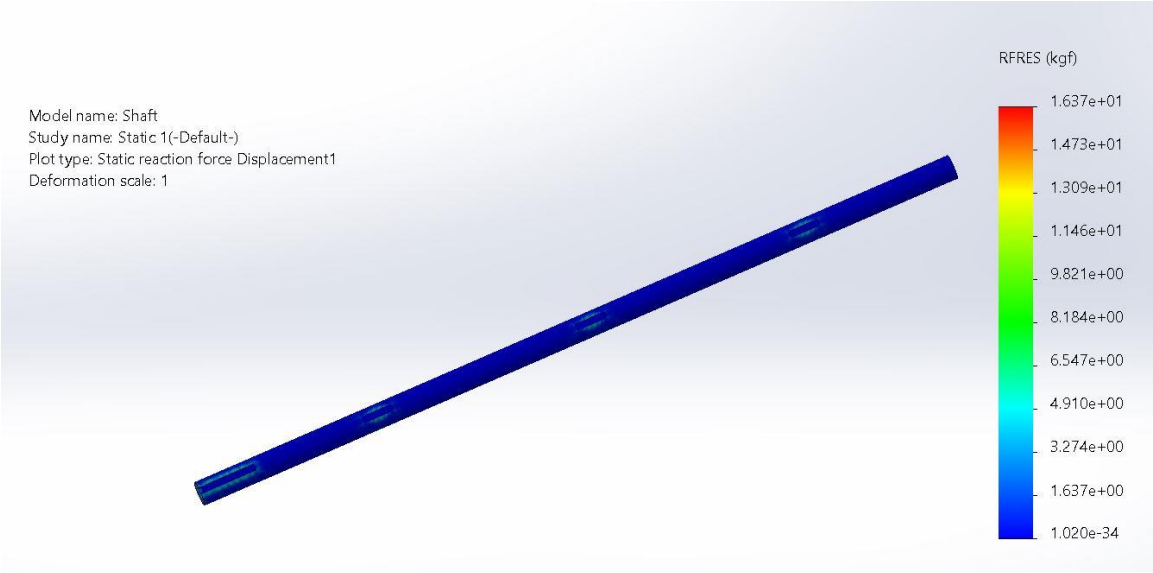

Fig.12. Shaft Finite Element Analysis Displacement Diagram.

For all analysis, minimum value location = fixed or supported points and maximum value location = high stress concentration points.

Parameter	Minimum Value	Maximum Value
Strain	7.244	7.3132
Stress	-8.559×10^{6} N/m^2	8.608×10^{6} N/m^2
Displacement	1.020 mm	1.637 mm

3.4.3. Finite element analysis of Pressure Gear

Based on the given sources, the detailed description of the analysis of gear strain, stress, safety, and displacement including the minimum and maximum values is provided:

Strain Analysis: determine the deformation behavior of the gear under the operational loads. The gear is modelled in 3D with the help of CAD software and imported into the FEA.

Minimum strain: The minimum strain typically occurs at the points where the gear is supported or fixed as these areas experience the minimum deformation.

Maximum strain: The maximum strain is found at the points of maximum stress concentration such as near the gear teeth where the contact forces are applied

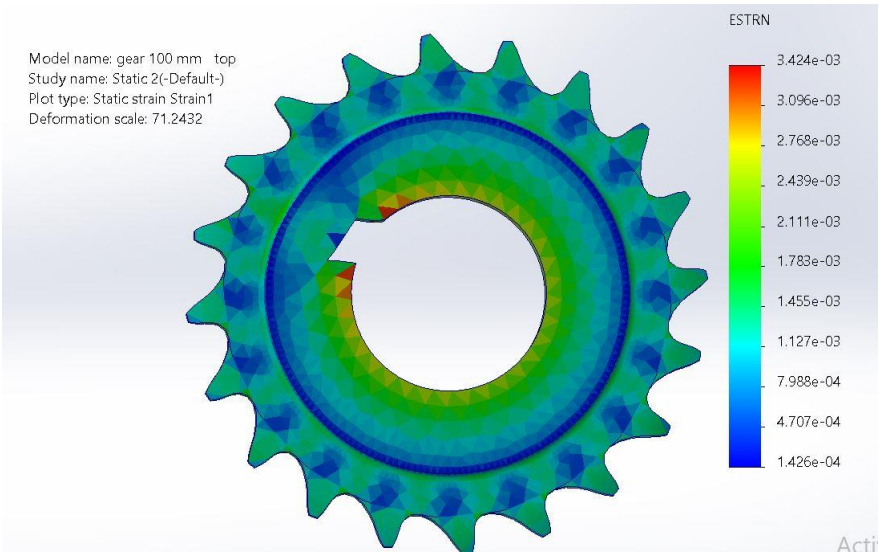

Fig.13. Gear Finite Element Analysis Stain Diagram.

Stress Analysis: To evaluate the distribution of stresses within the gear under the operational loads. The gear assembly is modeled and meshed with the appropriate elements.

Minimum stress: The minimum stress is found at the regions of the gear least affected by the applied loads such as the center of the gear which is far away from the point of application of the loads.

Maximum stress: The maximum stress is however found at the points of maximum loading such as the areas of the gear teeth and it can typically be measured.

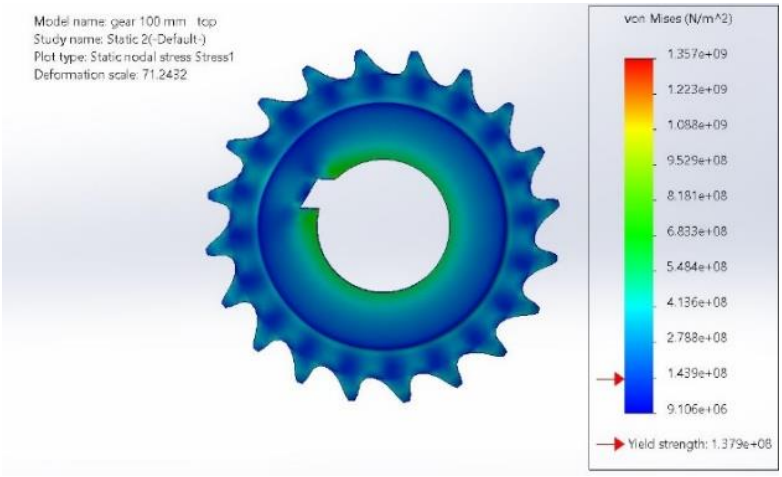

Fig.14. Gear Finite Element Analysis Stress Diagram.

Safety Factor Analysis: To ensure that the gear complies with the safe limits of usage under all expected loading conditions. The main purpose of the strain analysis is to determine the strain distribution on the gear surface and examine its excessive accumulation zones to prevent the risk of its failure.

Fig.15. Gear Finite Element Analysis Safety Diagram.

Minimum Safety Factor: The minimum safety factor is found at the points of maximum stress. A safety factor below 1 indicates potential failure, while a value above 1 indicates safe operation.

Maximum Safety Factor: The maximum safety factor is observed in regions with minimal stress, indicating a high margin of safety.

Displacement Analysis: The displacement of the gear under operational loads. The gear is modeled and meshed with appropriate.

Minimum Displacement: The minimum displacement occurs at the points where the gear is supported or fixed, as these areas are constrained from moving.

Maximum Displacement: The maximum displacement is observed at the free end of the gear or at the points of highest load application. This displacement is critical for ensuring that the gear does not interfere with other components or cause misalignment.

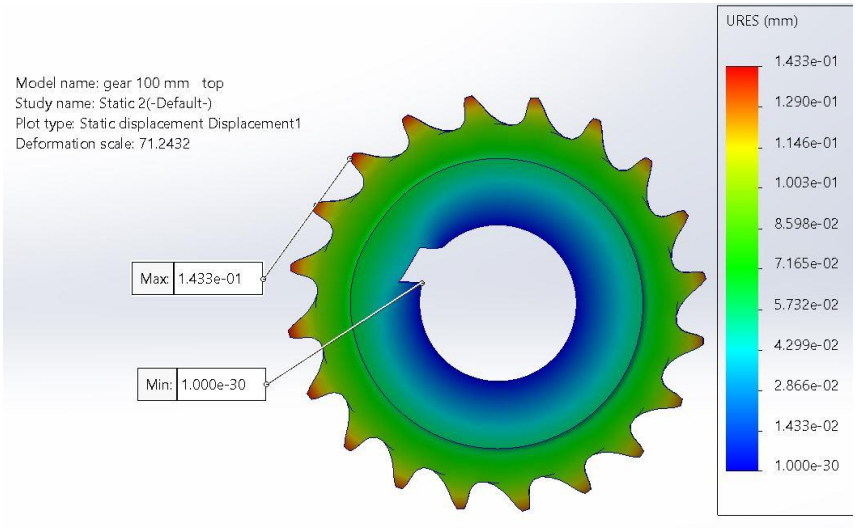

Fig.16. Gear Finite Element Analysis Displacement Diagram.

Table.1 Summary of Results.

Analysis Type	Minimum Value Location	Maximum Value Location
Strain	3.424	1.426
Stress	1.357×10^6 Nm2	1.379×10^6 Nm2
Safety Factor	1.016×10^6	1.514×10^6
Displacement	1.000 mm	1.433 mm

- Element analysis of conveyor belt shafts

A new study was undertaken to address weaknesses observed in the design of the shaft. Bearing clamps were carefully positioned at both ends of the shaft to maximize load distribution. Parameters including torque at the keyed joint and external forces such as centrifugal load and gravity were modeled precisely according to the shaft's rated rotational velocity. After meshing was complete, static stress analysis diagrams were calculated and their implications for structural integrity were probed deeply.

The makes abundantly clear, the finite element analysis stress diagram for the conveyor belt shaft indicates through its parameter values that when rotational force is imparted by the sprocket, regions of heightened stress form at the keyed connection and points where the shaft's diameter changes most abruptly. Moreover, the shaft's peak stress of 5.466×10^6 N/m^2 was reassuringly lower than its maximum rated breaking point of 2.939×10^8 N/m^2 under operating conditions.

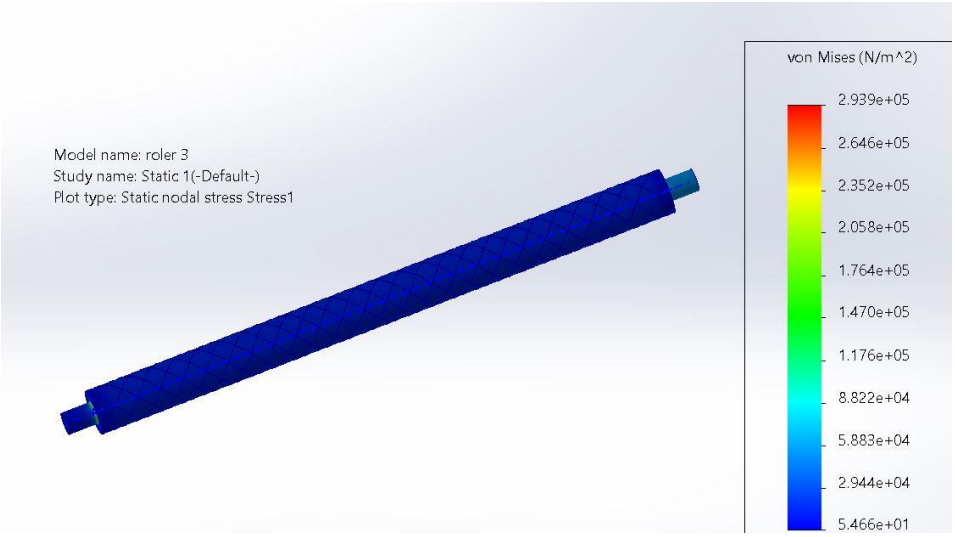

Fig.17. Stress Analysis.

The displacement diagram of the finite element analysis of the conveyor belt shaft as shown in through the displacement analysis diagram and the parameters on the right, it can be seen that under the working condition that the sprocket drives the shaft to rotate, the position of the larger displacement

on the shaft is in the middle of the shaft, the displacement at the maximum displacement on the shaft is 1.000mm, and the displacement is small within a reasonable range, which does not affect the normal use of the parts and meets the design requirements.

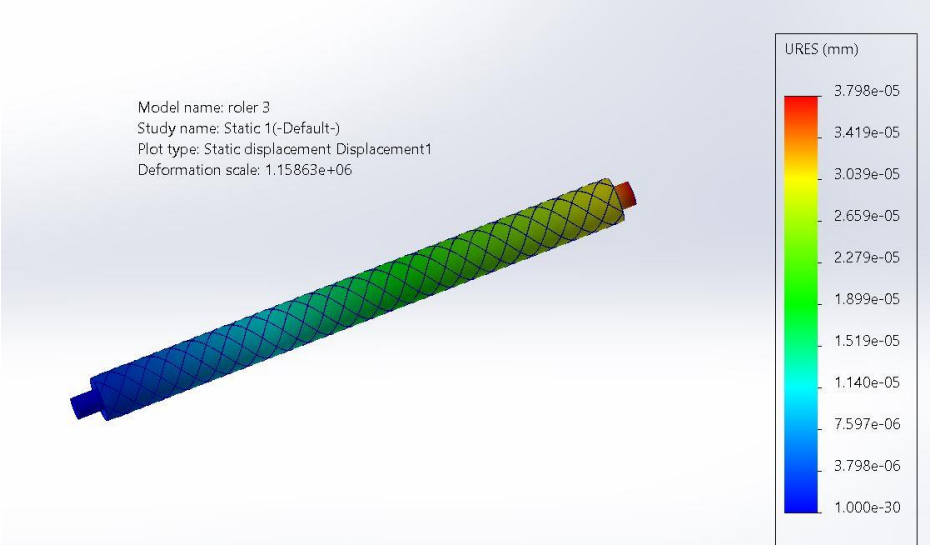

Fig.18. Displacement Analysis.

As shown in Figure 19, through the strain analysis diagram and the parameters on the right, it can be seen that under the working condition that the sprocket drives the shaft to rotate, the larger unit length deformation on the shaft is at the key connection and the shaft diameter change, the maximum unit length deformation on the shaft is 1.331, and strain value is very small and almost negligible, which meets the design requirements.

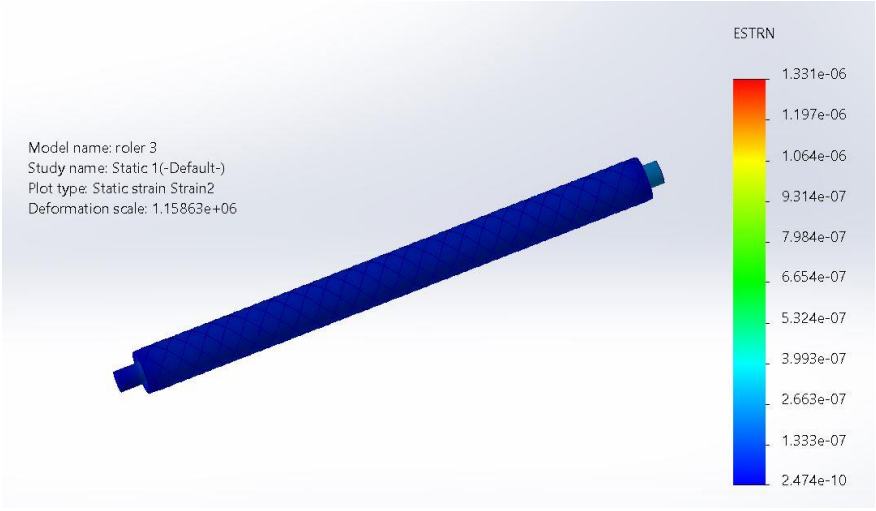

Fig.19. Strain Analysis.

The diagram of a safety factor of the shaft at the belt conveyor's finite-element analysis, it is possible to observe that the minimum safety factor at the maximum safety factor is $S=3.784\times10^{6}$. Moreover,

the combination of the following four results related to finite-element analysis enables to state that the shaft

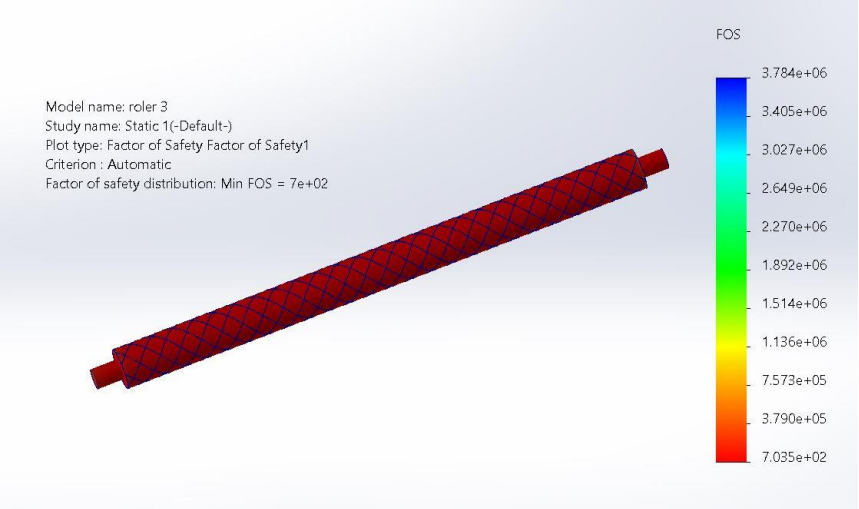

Fig.20. Safety Analysis.

Table 2. Manufacturing & Simulation Cost

Sr.NO.	Description	Quality	Rate	Amount
01	Material Cost	01	1,50,000/-	1,50,000/-
02	Machinhg Cost	01	50,000/-	50,000/-
03	Manufacturing Cost	01	50,000/-	50,000/-
04	Assembly Cost	01	10,000/-	10,000/-
05	Simulation Cost	01	15,000/-	15,000/-
			Total	2,25,000/-

9. Conclusion

The portable potato slicer designed in this study significantly enhances traditional slicing methods by offering superior productivity, flexibility, and safety. Unlike conventional slicers that are often bulky, costly, and inefficient with fixed blade settings, this modernized slicer provides adjustable slicing thickness and can process up to 1.5 tons per hour. By simply changing the blade holder, it can achieve slicing thicknesses of 0.5–0.7 mm, catering to a variety of processing needs.

Key design elements include the integration of a Dongles geared motor paired with a chain drive system that emulates manual slicing through a robust blade holder. Critical components such as shafts and bearings underwent thorough finite element analysis using SolidWorks, ensuring structural durability and operational efficiency. The slicer's food-contact parts are constructed from stainless

steel and SKD11 material, minimizing contamination risks and enhancing operator safety by reducing potential injury points .

While the slicer substantially decreases labor intensity and operational time, providing efficient and consistent slicing performance, there remains potential for further enhancements. Future iterations could explore additional automation features, improved energy efficiency, and integration with broader food processing systems. Overall, this design represents a significant advancement over traditional potato slicers, meeting both industrial and commercial processing demands with improved safety, performance, and adaptability.

References

[1] Yang Dan. Design and experimental study of pneumatic horizontal disc potato seeder[D]. Huazhong Agricultural University, 2016.

[2] Wen Jinli. Analysis on the impact of agrometeorological disasters on crop yield in China[J]. Rural Practical Science and Technology Information, 2021, 027(006):149-150.

[3] International Journal of Engineering Research & Technology (IJERT), Vol. 9, Issue 5, 2020.

[4] Sanni, L.A., & Olayanju, T.M. (2014). Design and Performance Evaluation of a Potato Slicer. Agricultural Engineering International: CIGR Journal, 16(3), 103-109.

[5] Journal of Food Engineering, 2021.

[6] Xie Zhongsheng.A review of the development of foreign slicers[J].Special Equipment for Electronic Industry,1996(03):36-42.

[7] Journal of Mechanical Design, ASME, 2018.

[8] Bhardwaj, R., & Kumar, N. (2015). Design Optimization of Potato Slicer Blade using Finite Element Analysis. International Journal of Mechanical Engineering and Technology (IJMET), 6(7), 45-54.

[9] Materials Science & Engineering A, Vol. 753, 2019..

[10] International Journal of Mechanical Engineering and Robotics Research, 2017.

[11] Wang Mingqiang, Zhu Yongmei. Beijing:Science Press,2016.

[12] Kale, A.P., & Patil, N.A. (2019). Mechanical Design and Automation of Potato Slicer Machine. International Journal of Mechanical and Production Engineering, 7(10), 152-160.